J. Earth Planet. Sci. Nagoya Univ., Vol. 57, 1 to 18, 2010

Radiolarian fossils from Quaternary gravel beds along the River Euphrates in Ar-Raqqa, Syria: A preliminary report

Manchuk NURAMKHAAN[1]*, Yusuke KATSURADA[2], Makoto SAITO[3], Kazuhiro TSUKADA[4], Mitsuo HOSHINO[5], Takeshi SAITO[6], Toshio NAKAMURA[7], Hidekazu YOSHIDA[4] and Tsuyoshi TANAKA[5]

[1]*School of Geology and Petroleum Engineering, Mongolian University of Science and Technology, Ulaanbaatar, Mongolia*
[2]*Center for Student Counseling, Nagoya University, Nagoya 464-8602, Japan*
[3]*AIST, Tsukuba 305-8567, Japan*
[4]*Nagoya University Museum, Nagoya 464-8601, Japan*
[5]*Graduate School of Environmental Studies, Nagoya University, Nagoya 464-8602, Japan*
[6]*Faculty of Science and Technology, Meijo University, Nagoya 468-8502, Japan*
[7]*Center for Chronological Research, Nagoya University, Nagoya 464-8602, Japan*
(Received July 9, 2010 / Accepted December 1, 2010)

ABSTRACT

Radiolarian fossils are here reported from clasts of pelagic chert in the Quaternary gravel beds along the River Euphrates in and around the Ghanem al-Ali, Ar-Raqqa, Syria. The gravel beds generally include clasts of silicified rock, felsic tuff and tuffaceous sandstone, rhyolite, quartzite, chert, plutonic rocks, metamorphic rocks and basalt. Minor amounts of sandstone, mudstone, limestone, gypsum etc. may also be present. Sixty-one percent of the chert samples include abundant radiolarian fossils of Middle Jurassic to Early Cretaceous age. This is a clear indication of the existence of Middle Jurassic to Lower Cretaceous radiolarian chert in the eastern Taurides, upriver regions of the River Euphrates. Such exposures have not previously been reported in the eastern Taurides.

INTRODUCTION

The Alpine orogenic belt that divides the African-Arabian from the Eurasian composite cratons is a key to understanding the evolution of the Tethyan ocean. The southern Alpine orogenic belt in the Middle East is divided into the Pontides in the north and the Anatolide-Tauride block in the south (Fig. 1). The Pontides is considered to be a convergent zone of the Paleo-Tethys (Şengör, 1979; Şengör and Yilmaz, 1981) and is bounded to the south by the Izmir-Ankara, Ankara-Erzincan and Sevan-Akera sutures (Fig. 1). The Pontides is lithologically subdivided into the Istanbul and Sakarya zones (Fig. 1, Murat, 1993). The Kirşehir massif is embedded between the Pontides and the Anatolide-Tauride block as a continental fragment within central Turkey. The Anatolide-Tauride block is composed of continental fragments along with piles of nappes from sedimentary-igneous rock complexes (e.g. Murat, 1993; Okey, 1984,

*Corresponding author, e-mail: manchukn@gmail.com

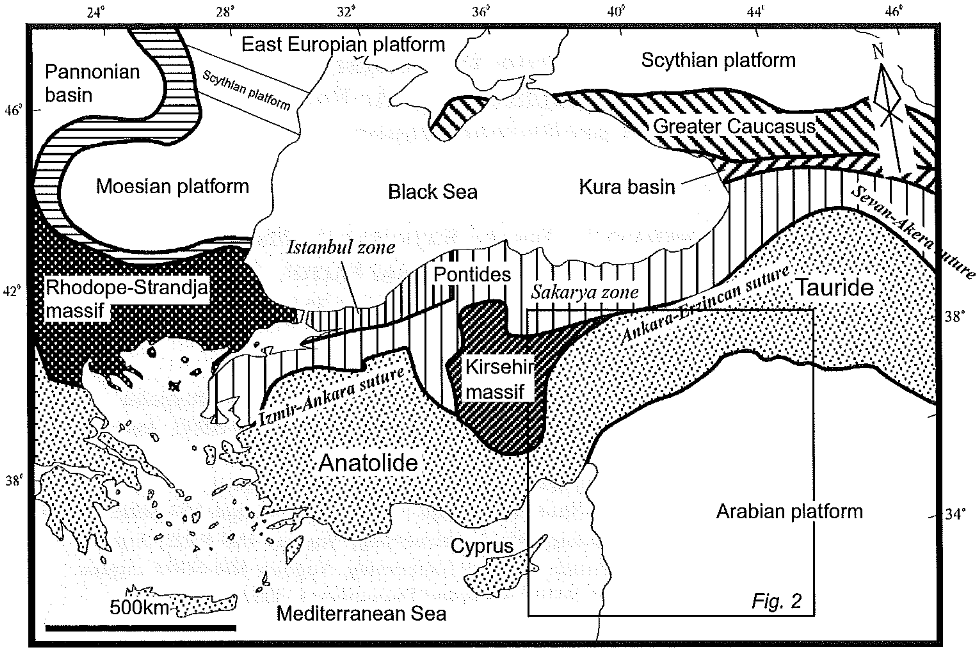

Fig. 1 Tectonic division of the Alpine orogenic belt in the Middle East and southeastern Europe.

1985; Şengör and Yilmaz, 1981) and is considered to be a remnant of the Neo-Tethys (Şengör, 1979; Şengör and Yilmaz, 1981).

The age and distribution of rocks in the Anatolide-Tauride block, south Turkey, are important factors in revealing the tectonic process of the Alpine orogeny, and various studies have been made on the Anatolide and western Taurides (e.g. Demirtasli, 1984; Dewey *et al.*, 1986; Göncüoglu and Turhan, 1984; Hall, 1976; Ozgul, 1984; Robertson and Woodcook, 1981; Şengör and Yilmaz, 1981; Tekeli *et al.*, 1984; Woodcook and Robertson, 1982). Although some studies on stratigraphy and structure, for example on the Munzur-Keban-Baskil nappes, have been made in the eastern Taurides, there is still more work to do on the lithology and age of pelagic sedimentary rocks there. Radiolarian chert, which has accumulated in a deep ocean basin of the Tethys, is commonly incorporated in accretionary complexes related to the subduction of ocean crust (Robertson, 2002). The age of radiolarians from such accretionary complexes provides valuable upper and lower limits to the timing of related geological processes, including spreading and tectonic accretion (e.g. Al Riyami *et al.*, 2001; Beccaletto *et al.*, 2005). However, geological and paleontological data from the radiolarian chert in the Anatolide-Tauride block are still limited.

Radiolarian chert dated to the Triassic to Cretaceous has recently been reported from the Pontides, Anatolide and western Taurides as evidence of the fossilized remains of the Tethyan ocean (e.g. Bozkurt *et al.*, 1997; Danelian *et al.*, 2006; De Wever *et al.*, 1979; Göncüoglu *et al.*, 2004, 2006; Mekik, 2000; Nikita and Tekin, 1996; Tekin and Göncüoglu, 2008, 2009; Tekin, *et al.*, 2002). Although outcrops of radiolarian chert are also known in the eastern Taurides (Geological Survey of Turkey, 1963, 1966,

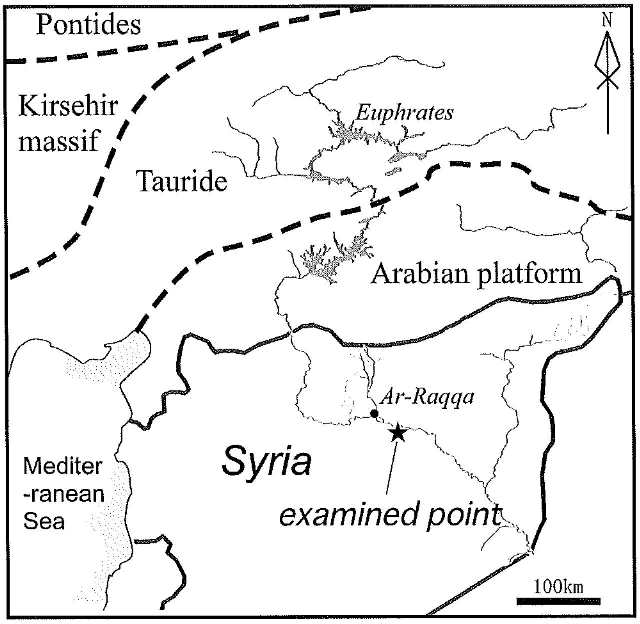

Fig. 2 Index map of the examined area. The River Euphrates and the tectonic division of southern Turkey are also shown.

1975, 1989, and 2002a, b, and c), very few attempts have been made at equivalent studies there.

This paper is a preliminary report on the radiolarian fossils from clasts of pelagic chert in the Quaternary gravel beds along the River Euphrates in and around the Ghanem al-Ali, Ar-Raqqa, Syria in due course of an archaeological study. Clasts examination is a convenient way to know the geological outline of broad area of upper reaches of the river, and the radiolarians give us useful information on the age distribution of pelagic chert in the eastern Taurides. This is an initial step in broader examination of the radiolarian chert in the eastern Tauride in the upper reaches of the river (Fig. 2)

GEOLOGY IN AND AROUND THE GHANEM AL-ALI

The area in and around Ghanem al-Ali has exposures of Neogene sedimentary rocks and Quaternary sediments and basalts (Ministry of Industry, S.A.R., 1964). The Neogene sedimentary rocks form the Bishri Plateau and consist mainly of gypsum with fine-grained felsic tuff intercalations (Fig. 3). The Quaternary sediments are composed of well-stratified silts, sands and gravels and overlie the Neogene sedimentary rocks abutting them with unconformity (Fig. 3). The bedding planes of these sedimentary rocks and sediments are sub-horizontal. The basalts are dated as 1.38 to 2.72 K-Ar ages and are composed of Pahoehoe- and Aa-lava and pyroclastic rocks and they form conical volcanic bodies. Details of the Neogene sedimentary rocks and the Quaternary sediments are described below.

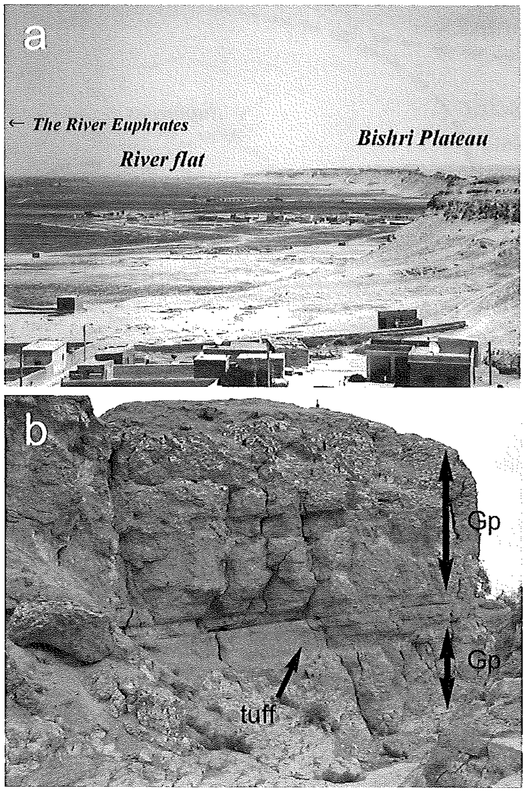

Fig. 3 Photographs of distant view of the Ghanem al-Ali (a) and rocks forming the Bishri Plateau (b). The photograph (a) was by Mr. T. Kiuchi (Ohnuma *et al.*, 2008).

(1) Neogene sedimentary rocks

The sedimentary rocks, which are more than 70 m thick, are mainly composed of coarse, crystalline, white to gray gypsum. The gypsum is partly stratified with layers 10 to 20 cm thick. Milky white, pale green and pale blue, fine-grained felsic tuff layers, 10 cm to 3 m thick, are intercalated in the gypsum in some horizons. The felsic tuff is generally well stratified. Abundant foraminifera, bivalve and other fossils are included in the felsic tuff layers in some places. Gypsum veins and globular nodules are developed in the layers. The same kind of felsic tuff is intensely silicified in the Bir-Sbai, 50km south of the Ghanem al-Ali. The gypsum and felsic tuff in the Ghanem al-Ali are sub-horizontal, but they are folded with horizontal axes and vertical axial planes, dozens kilometers of half-wavelength at the Hawijat shnan. The sedimentary rocks are assigned to the upper Middle Miocene (Ministry of Industry, S.A.R., 1964).

(2) Quaternary sediments

The Quaternary sediments are made up of alternating beds of silt, sand and gravel and overlie the Neogene sedimentary rocks which they abut with unconformity. The sediments form five levels of terraces along the River Euphrates (Fig. 4a, Hoshino *et al.*, 2010) and can be divided into two types by their lithostratigraphy: Lower unit

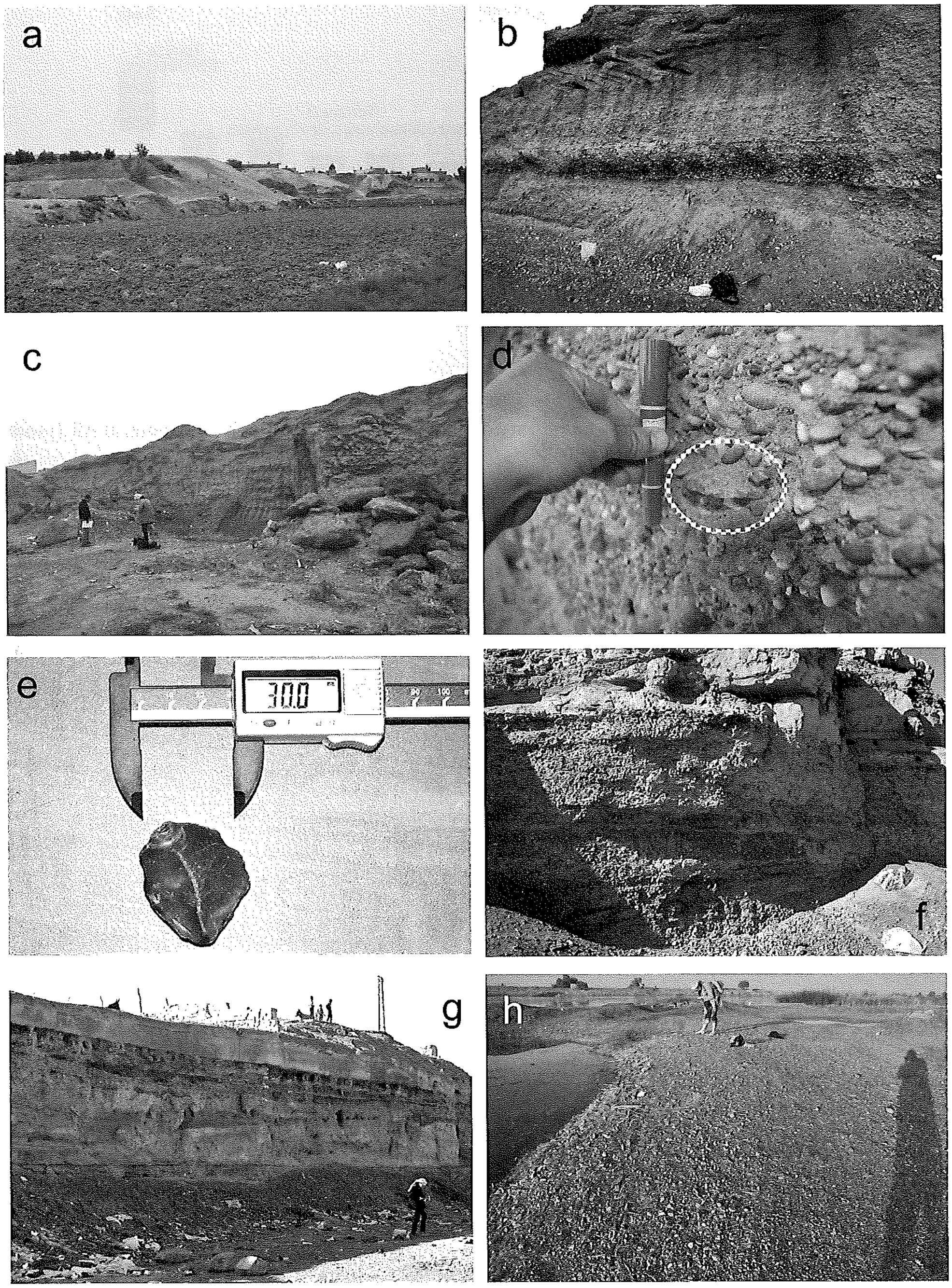

Fig. 4 Photographs of the sampling localities. (a): River terrace exposing the Quaternary sediments along the River Euphrates. Localities A to D are on the bank of river terraces of this kind. (b): A photograph of Locality A. (c) and (d): Photographs of Locality B. The gravel beds commonly include clasts of stone tools. The dotted circle in (d) shows how stone tools occur. (e): A stone tool from the gravel beds. (f): A photograph of Locality C. (g): A photograph of Locality D. (h): A photograph of Locality E. Locality E is on the bank of the River Euphrates.

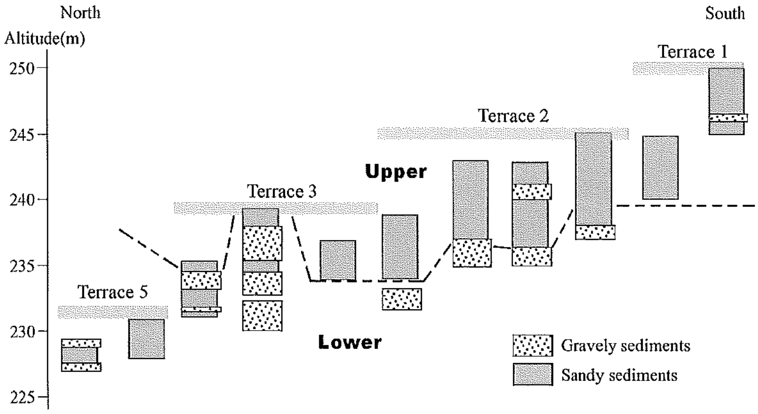

Fig. 5 Columnar sections of the Quaternary sediments in and around the Ghanem al-Ali (modified from Hoshino *et al.*, 2010).

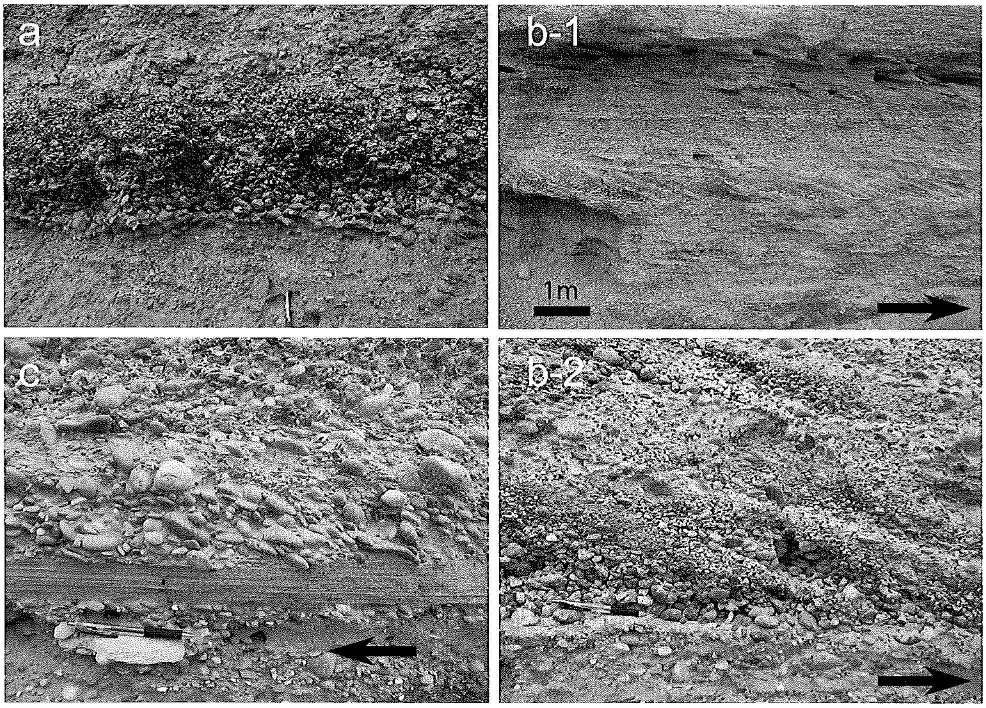

Fig. 6 Close-up views of the gravel beds. The gravel beds exhibit various kinds of sedimentary structures. (a): A photograph showing graded bedding. (b): Cross bedding indicating an eastward-flowing paleo-current (b-1) and graded beddings (b-2). Black arrows show current direction. (c): Imbrications of flattened clasts showing an eastward-flowing paleo-current. Black arrow shows current direction.

composed largely of alternating beds of grey fine to course sand and gravel, and Upper unit composed mainly of milky- to yellowish- white silt and sand with minor intercalations of gravel beds (Fig. 5).

The sediments of Lower unit are generally well stratified with various kinds of sedimentary structures such as graded-bedding, cross-bedding and clast imbrications (Fig. 6). An eastward-flowing paleo-current is indicated by the sedimentary structures. The gravel beds are composed mostly of well-rounded flattened clasts of red chert, plutonic rocks, felsic volcanic rocks, basalt, metamorphic rocks and silicified rocks, several millimeters to ca. 10 cm across. They are generally clast-supported and well sorted. Stone tools from the Lower Paleolithic (personal communication with Prof. Nishiwaki at Tokyo University) are included in the gravel beds as clasts (Fig. 4d, e), so the sediments must be more recent than the Lower Paleolithic.

SAMPLING METHOD

Five hundreds and ninety-two samples of clasts from 5 points along the River Euphrates in Ar-Raqqa were examined (Figs. 4 and 7). At Localities A to D the Quaternary gravel beds of the Lower Unit are well exposed on terrace banks between the Ghanem al-Ali and the Zor Shammar (Fig. 7). These localities are on the flood plain about 4 km away from the River Euphrates. Locality E is on the bank of the Euphrates about 11 km ENE from the Ghanem al-Ali (Fig. 7).

Clasts with diameters greater than 5mm were sampled randomly in such a way that they fully fill a plastic bag (40 × 28 cm) at each of the five localities. Samples at Localities A to D were from the Quaternary gravel beds, and those at Locality E were from floodplain deposits at the riverbank.

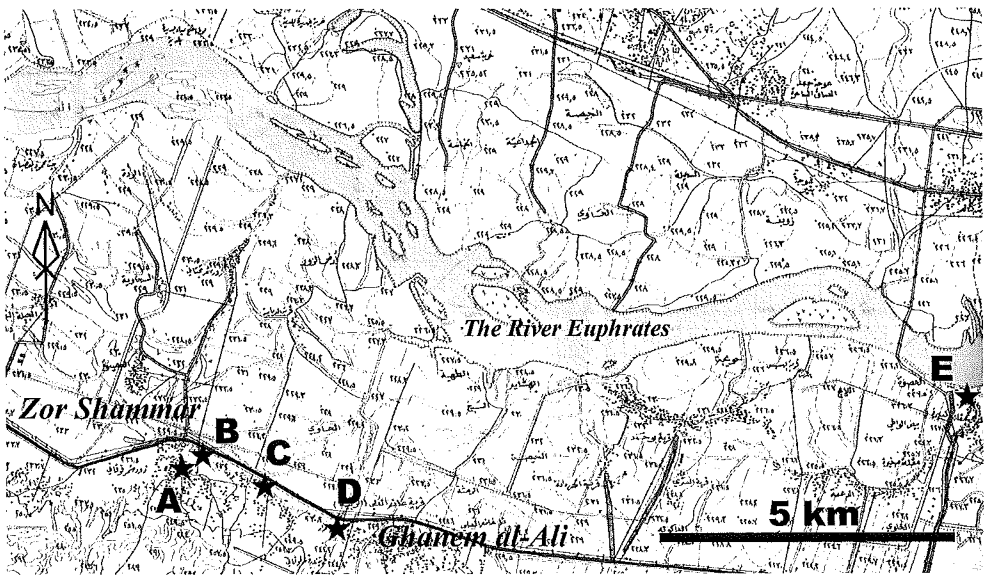

Fig. 7 Sampling localities of clasts. The area is shown in Fig. 2.

Table 1. Clast composition of gravel beds at Localities A to E.

Loc. A N = 133

diamet.	S.R.	Tuff	Tuff Ss.	Rhy.	Ms.	Ss.	Bs.	Ls.	Rad. Ch.	Ch.	Gyp.	Qtz.	Plu-ton.	Meta-ch.	Meta-Ss.	Meta-Bs.	Gn.	Other	Total
>5 cm	18	11	0	5	0	0	2	0	2	0	0	4	3	4	0	0	0	0	49
3–5 cm	2	5	0	3	1	2	1	1	1	2	0	6	2	0	0	0	0	0	26
2–3 cm	2	9	0	3	0	0	0	0	1	1	0	2	4	1	0	0	0	1	24
<2 cm	1	6	0	4	2	1	2	1	1	4	0	5	5	1	0	0	1	0	34
Total	23	31	0	15	3	3	5	2	5	7	0	17	14	6	0	0	1	1	133
%	17.3%	23.3%	0.0%	11.3%	2.3%	2.3%	3.8%	1.5%	3.8%	5.3%	0.0%	12.8%	10.5%	4.5%	0.0%	0.0%	0.8%	0.8%	100.0%

Loc. B N = 123

diamet.	S.R.	Tuff	Tuff Ss.	Rhy.	Ms.	Ss.	Bs.	Ls.	Rad. Ch	Ch.	Gyp.	Qtz.	Plu-ton.	Meta-ch.	Meta-Ss.	Meta-Bs.	Gn.	Other	Total
>5 cm	7	10	0	4	0	0	8	1	9	5	0	8	2	5	0	0	2	0	61
3–5 cm	1	4	0	2	0	0	1	1	5	0	0	2	5	7	0	0	1	0	29
2–3 cm	3	2	0	1	1	1	1	1	0	1	0	6	7	0	0	0	2	0	26
<2 cm	0	3	0	1	0	0	0	0	0	1	0	2	0	0	0	0	0	0	7
Total	11	19	0	8	1	1	10	3	14	7	0	18	14	12	0	0	5	0	123
%	8.9%	15.4%	0.0%	6.5%	0.8%	0.8%	8.1%	2.4%	11.4%	5.7%	0.0%	14.6%	11.4%	9.8%	0.0%	0.0%	4.1%	0.0%	100.0%

Loc. C N = 70

diamet.	S.R.	Tuff	Tuff Ss.	Rhy.	Ms.	Ss.	Bs.	Ls.	Rad. Ch.	Ch.	Gyp.	Qtz.	Plu-ton.	Meta-ch.	Meta-Ss.	Meta-Bs.	Gn.	Other	Total
>5 cm	14	7	1	4	1	2	6	1	3	11	0	8	1	5	0	0	0	0	64
3–5 cm	0	0	0	0	0	1	0	0	1	1	0	1	0	0	0	0	0	0	4
2–3 cm	0	0	0	0	0	0	0	0	1	1	0	0	0	0	0	0	0	0	2
<2 cm	0	0	0	0	0	0	0	0	0	0	0	0	0	0	0	0	0	0	0
Total	14	7	1	4	1	3	6	1	5	13	0	9	1	5	0	0	0	0	70
%	20.0%	10.0%	1.4%	5.7%	1.4%	4.3%	8.6%	1.4%	7.1%	18.6%	0.0%	12.9%	1.4%	7.1%	0.0%	0.0%	0.0%	0.0%	100.0%

Loc. D N = 185

diamet.	S.R.	Tuff	Tuff Ss.	Rhy.	Ms.	Ss.	Bs.	Ls.	Rad. Ch.	Ch.	Gyp.	Qtz.	Plu-ton.	Meta-ch.	Meta-Ss.	Meta-Bs.	Gn.	Other	Total
>5 cm	2	5	0	10	0	3	3	1	4	2	0	9	6	18	1	1	2	0	67
3–5 cm	0	22	0	9	0	2	8	1	7	5	0	8	7	3	3	0	0	0	75
2–3 cm	3	2	0	6	0	0	2	0	3	2	2	5	6	2	0	0	0	0	33
<2 cm	0	1	0	1	0	0	3	0	2	0	0	2	0	1	0	0	0	0	10
Total	5	30	0	26	0	5	16	2	16	9	2	24	19	24	4	1	2	0	185
%	2.7%	16.2%	0.0%	14.1%	0.0%	2.7%	8.6%	1.1%	8.6%	4.9%	1.1%	13.0%	10.3%	13.0%	2.2%	0.5%	1.1%	0.0%	100.0%

Loc. E N = 81

diamet.	S.R.	Tuff	Tuff Ss.	Rhy.	Ms.	Ss.	Bs.	Ls.	Rad. Ch.	Ch.	Gyp.	Qtz.	Plu-ton.	Meta-ch.	Meta-Ss.	Meta-Bs.	Gn.	Other	Total
>5 cm	12	6	0	4	0	4	5	0	6	3	0	3	0	10	2	0	1	1	57
3–5 cm	7	2	0	1	0	1	0	0	5	1	0	3	0	3	0	0	0	0	23
2–3 cm	0	0	0	0	0	0	0	0	1	0	0	0	0	0	0	0	0	0	1
<2 cm	0	0	0	0	0	0	0	0	0	0	0	0	0	0	0	0	0	0	0
Total	19	8	0	5	0	5	5	0	12	4	0	6	0	13	2	0	1	1	81
%	23.5%	9.9%	0.0%	6.2%	0.0%	6.2%	6.2%	0.0%	14.8%	4.9%	0.0%	7.4%	0.0%	16.0%	2.5%	0.0%	1.2%	1.2%	100.0%

TOTAL N = 592

diamet.	S.R.	Tuff	Tuff Ss.	Rhy.	Ms.	Ss.	Bs.	Ls.	Rad. Ch.	Ch.	Gyp.	Qtz.	Plu-ton.	Meta-ch.	Meta-Ss.	Meta-Bs.	Gn.	Other	Total
>5 cm	53	39	1	27	1	9	24	3	24	21	0	32	12	42	3	1	5	1	298
3–5 cm	10	33	0	15	1	6	10	3	19	9	0	20	14	13	3	0	1	0	157
2–3 cm	8	13	0	10	1	1	3	1	6	5	2	13	17	3	0	0	2	1	86
<2 cm	1	10	0	6	2	1	5	1	3	5	0	9	5	2	0	0	1	0	51
Total	72	95	1	58	5	17	42	8	52	40	2	74	48	60	6	1	9	2	592
%	12.2%	16.0%	0.2%	9.8%	0.8%	2.9%	7.1%	1.4%	8.8%	6.8%	0.3%	12.5%	8.1%	10.1%	1.0%	0.2%	1.5%	0.3%	100.0%

S.R.: silicified rock, Ss.; sandstone, Rhy.: rhyolite, Ms.: mudstone, Bs.: basalt, Ls.: limestone, Rad. Ch.: radiolarian chert, Ch.: chert without radiolarians, Gyp.: gypsum, Qtz.: quartzite, Pluton.: plutonic rocks, Meta-ch.: meta-chert, Meta-Ss.: meta-sandstone, Meta-Bs.: meta-basalt, Gn.: gneiss.

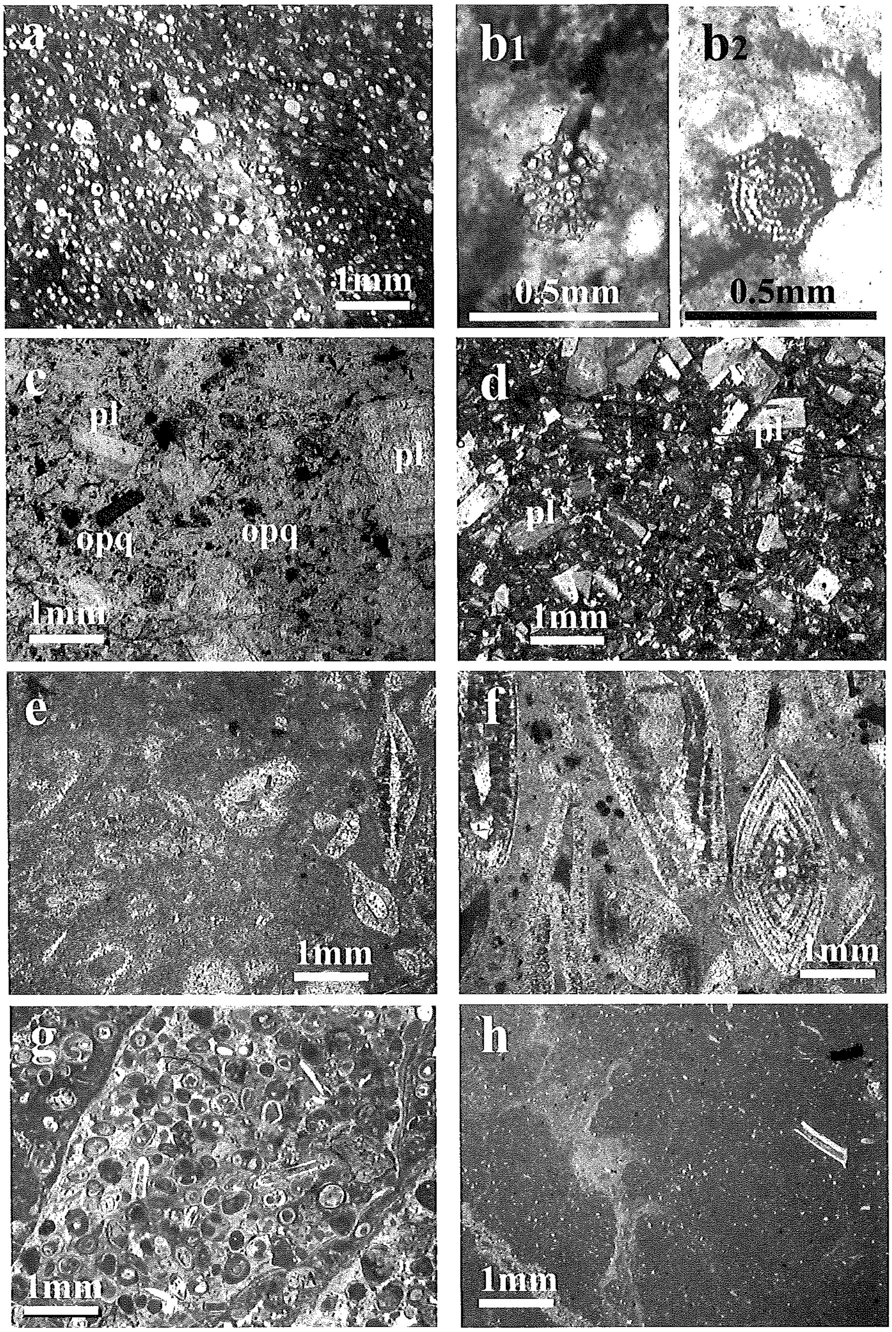

Fig. 8-1 Photomicrographs of clasts and silicified tuff. (a) Radiolarian chert (sample No. sy 5). Plane polarized light. (b) Radiolarian fossils in sample No. sy 5. (c) Rhyolite from Locality D. Plane polarized light. (d) Felsic tuff from Locality D. Crossed polars. (e) Silicified rock including abundant fossils from Locality D. Plane polarized light. (f) Silicified rock from Locality D. Crossed polars. (g) Silicified tuff including many fossils from the Bir-Sbai. Crossed polars. (h) Micritic limestone from Locality D. Plane polarized light.

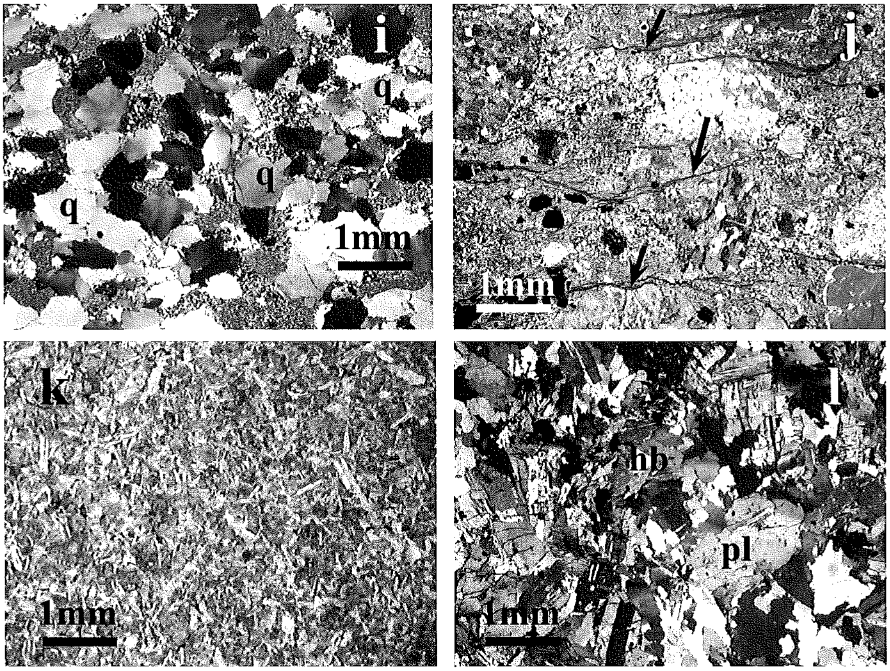

Fig. 8-2 Photomicrographs of clasts. (i) Meta-sandstone from Locality D. Crossed polars. (j) Gneiss from Locality D. Crossed polars. Arrows show planes defined by preferred orientation of mica. (k) Basalt from Locality C. Plane polarized light. (l) Plutonic rock from Locality C. Crossed polars. Q: quartz, pl: plagioclase, hb: hornblend.

PETROLOGY OF THE CLASTS

The gravel beds include clasts of silicified rock (12%), felsic tuff and tuffaceous sandstone (16%), rhyolite (10%), quartzite (13%), chert (16%), plutonic rocks (8%), metamorphic rocks (10%) and basalt (7%) as major components, and minor amounts of sandstone (3%), mudstone (1%), limestone (1%), gypsum (0.3%) and others (0.3%) (Table 1). The clasts of silicified rock, rhyolite and chert, over ca. 3 cm across, generally have percussion marks on their surface. The chert clasts are mostly red and 61% of them include abundant radiolarian fossils (Fig. 8a, b and Table 1). Some radiolarian chert samples also yield foraminifera (Fig. 9). The phenocrysts in the rhyolite are euhedral to subhedral plagioclase with scattered flakes of opaque minerals which lie in a matrix of cryptocrystalline quartz, plagioclase and secondary minerals (Fig. 8c). The felsic tuff contains many fine- to medium-sized angular fragments and crystals of felsic volcanic origin (Fig. 8d). The silicified rock is generally composed of cryptocrystalline quartz, and 9% include abundant foraminifera, bivalves etc. (Fig. 8e, f). Radiolarians are rarely included in the silicified rock. Some of the silicified rock includes abundant needles of small plagioclase. The metamorphic rocks originate from chert, sandstone, basalt and plutonic rock (Fig. 8i, j), are the most abundant. The metamorphic rocks of sandstone and plutonic rock origin show foliation defined by parallel arrangement of mica minerals (Fig. 8j). The meta-chert is entirely composed

Locality	No.	Fossil	Rock type
Loc. A	*sy 16*	*Archaeospongoprunum* sp.	*chert*
Loc. B	*sy 5*	*Pseudodictyomitra* sp. *Homoeoparonaella* sp. foraminifera	*chert*
	sy 7	*Archaeodictyomitra* sp. Pantanelliidae gen. et sp. indet.	*chert*
	sy 12	*Thanarla* sp.	*chert*
	sy 9	*Hsuidae gen. et* sp. *indet.* foraminifera	*silicified rock*
Loc. D	*sy 51*	*Parvicingula* cf. *dhimenaensis* Eucyrtidiellidae gen. et sp. indet.	*chert*
	sy 52	*Archaeodictyomitra* sp. *Acaeniotyle umbilicata* *Thanarla* sp.	*chert*
	sy 55	*Praeconosphaera* cf. *sphaeraconus* *Pseudodictyomitra* aff. *lanceloti*	*chert*
	sy 58	*Homoeoparonaella* sp. *Pseudodictyomitra leptoconica* *Pantanellium squinaboli* *Spongotripus* (?) sp. Archaeodictyomitridae gen. et sp. indet.	*chert*
Loc. E	*sy 20*	*Pantanellium oligoporum* *Poulpus* sp.	*chert*
	sy 25	foraminifera	*chert*
	sy 29	*Mirifusus* cf. *dianae*	*chert*
	sy 32	foraminifera	*silicified rock*

Fig. 9 A list of fossils from gravel bed clasts.

of microcrystalline quartz. The basalt generally has an intersertal texture and most of the minerals, except for plagioclase and clinopyroxene, are largely replaced by secondary minerals such as muscovite, chlorite and calcite (Fig. 8k). The plutonic rock is composed mainly of plagioclase and hornblend with a subordinate amount of quartz (Fig. 8l).

RADIOLARIAN FOSSILS FROM THE CLASTS

Radiolarians and foraminifera were obtained from clasts of chert (11 samples) and silicified rock (2 samples) (Fig. 9 and Plate 1). The species identified are *Archaeodictyomitra* sp., *Archaeospongoprunum* sp., *Acaeniotyle umbilicata* (Ruest), *Homoeoparonaella* sp., *Mirifusus* cf. *dianae* (Karrer), *Pantanellium oligoporum* (Vinassa), *Pantanellium squinaboli* (Tan), *Parvicingula* cf. *dhimenaensis* Baumgartner, *Poulpus* sp., *Praeconosphaera* cf. *sphaeraconus* (Ruest), *Pseudodictyomitra leptoconica* (Foreman), *Pseudodictyomitra* aff. *lanceloti* Schaaf, *Pseudodictyomitra* sp., *Spongotripus* (?) sp., *Thanarla* sp., Archaeodictyomitridae gen. et sp. indet., Eucyrtidiellidae gen. et sp. indet., Hsuidae gen. et sp. indet., Pantanelliidae gen. et sp. indet. These radiolarians suggest Jurassic to Cretaceous age. Details are as follows:

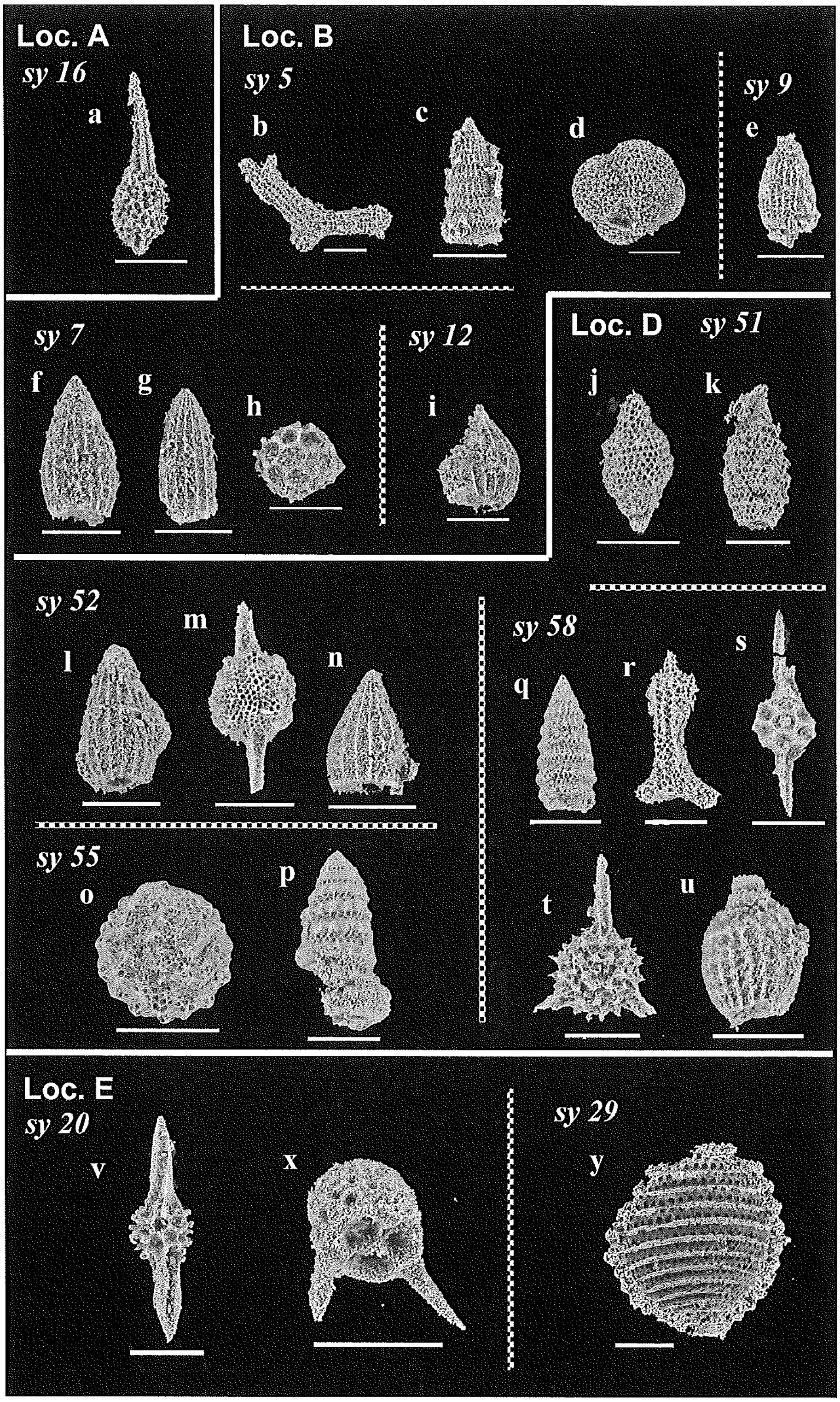
Loc. A
sy 16
a
Loc. B
sy 5
b
c
d
sy 9
e
sy 7
f
g
h
sy 12
i
Loc. D
sy 51
j
k
sy 52
l
m
n
sy 58
q
r
s
sy 55
o
p
t
u
Loc. E
sy 20
v
x
sy 29
y

Plate 1

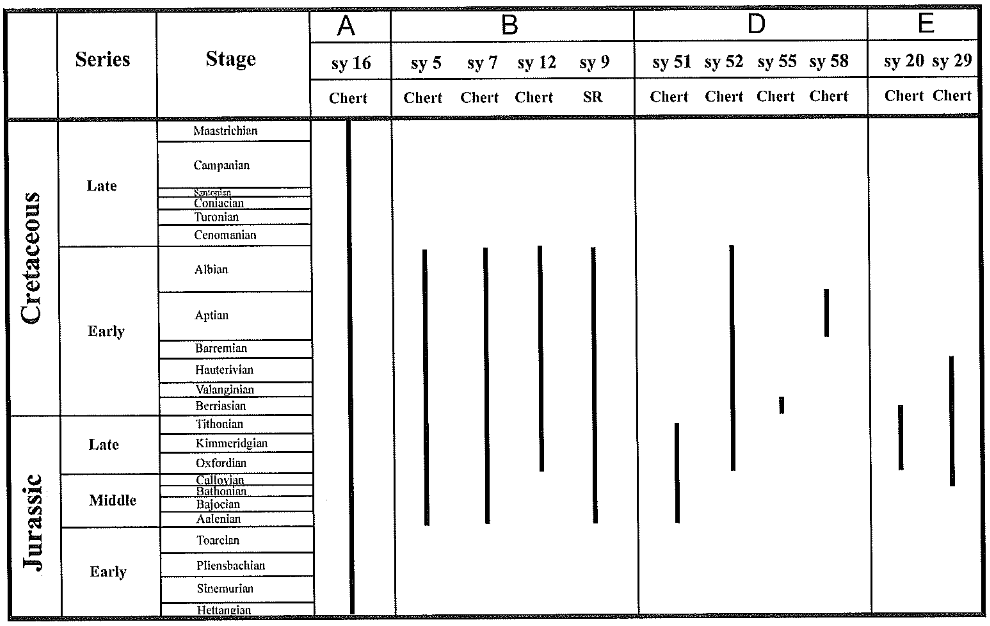

Fig. 10 Range chart of radiolarian fossils.

(1) Locality A

Sample No. sy 16 (chert): *Archaeospongoprunum* sp. was obtained from a chert clast (Fig. 9 and Plate 1). The genus *Archaeospongoprunum* is generally known from Jurassic or older to Cretaceous, however Clark and Campbell (1942) described *Spongoprunum markleyense* which maybe included in the genus *Archaeospongoprunum* from the Eocene of California (Pessagno, 1973). The age of the gravel is therefore Jurassic to Cretaceous or possibly Eocene (Fig. 10).

(2) Locality B

Sample No. sy 5 (chert): A chert clast yielded *Pseudodictyomitra* sp. and *Homoeoparonaella* sp. (Fig. 9 and Plate 1). The genus *Pseudodictyomitra* ranges from Middle Jurassic to Late Cretaceous (O'Dogherty, 1994) and the genus *Homoeoparonaella* ranges from Callovian (?) to Aptian (Baumgartner, 1980). The clast is therefore Middle Jurassic to Early Cretaceous (Fig. 10). Foraminifera were also extracted from this clast.

Sample No. sy 7 (chert): A chert clast yielded *Archaeodictyomitra* sp. and

---

Plate 1. Radiolarian fossils and foraminifera from the clasts. Scale bars denote 100 μm

(Locality A)
a. *Archaeospongoprunum* sp.
(Locality B)
b. *Homoeoparonaella* sp.
c. *Pseudodictyomitra* sp.
d. foraminifera
e. Hsuidae gen. et sp. indet.
f. *Archaeodictyomitra* sp.
g. *Archaeodictyomitra* sp.
h. Pantanelliidae gen. et sp. indet.
i. *Thanarla* sp.
(Locality D)
j. Eucyrtidiellidae gen. et sp. indet.
k. *Parvicingula* cf. *dhimenaensis* Baumgartner
l. *Archaeodictyomitra* sp.
m. *Acaeniotyle umbilicata* (Ruest)
n. *Thanarla* sp.
o. *Praeconosphaera* cf. *sphaeraconus* (Ruest)
p. *Pseudodictyomitra* aff. *lanceloti* Schaaf
q. *Pseudodictyomitra leptoconica* (Foreman)
r. *Homoeoparonaella* sp.
s. *Pantanellium squinaboli* (Tan)
t. *Spongotripus* (?) sp.
u. Archaeodictyomitridae gen. et sp. indet.
(Locality E)
v. *Pantanellium oligoporum* (Vinassa)
x. *Poulpus* sp.
y. *Mirifusus*. cf. *dianae* (Karrer)

Pantanelliidae gen. et sp. indet. (Fig. 9 and Plate 1). The *Ad.* sp. here is similar to *Ad.* sp. 8 described in Hori *et al.* (2002). The genus *Archaeodictyomitra* ranges from Middle Jurassic to Late Cretaceous (Pessagno, 1977; O'Dogherty, 1994). The family Pantanelliidae is known from the Carnian to the Aptian (De Wever *et al.*, 2001). Thus the age of the clast is Middle Jurassic to Early Cretaceous (Fig. 10).

Sample No. sy 12 (chert): A chert clast yielded *Thanarla* sp. (Fig. 9 and Plate 1) similar to *T. brouweri* (TAN) which is know from Upper Jurassic to Lower Cretaceous (Baumgartner *et al.*, 1995a, b, Fig. 10)

Sample No. sy 9 (silicified rock): Hsuidae gen. et sp. indet. ranging from Early Jurassic to Early Cretaceous (De Wever *et al.*, 2001) were extracted from a clast of silicified rock (Figs. 9 and 10 and Plate 1). This clast also yielded foraminifera.

(3) Locality D

Sample No. sy 51 (chert): *Parvicingula* cf. *dhimenaensis* and Eucyrtidiellidae gen. et sp. indet. were obtained from a chert clast (Fig. 9 and Plate 1). Baumgartner *et al.* (1995a, b) showed that *Pvc. dhimenaensis* ranges from Middle to Late Jurassic. Therefore, it is likely that the age of this sample is Middle to Late Jurassic (Fig. 10).

Sample No. sy 52 (chert): A chert clast yielded *Archaeodictyomitra* sp., *Acaeniotyle umbilicata* and *Thanarla* sp. (Fig. 9 and Plate 1). This *Ad.* sp. resembles *Ad.* sp. 8 described in Hori *et al.* (2002). The genus *Archaeodictyomitra* ranges from Middle Jurassic to Late Cretaceous (Pessagno, 1977). According to Baumgartner *et al.* (1995a, b), *Ac. umbilicata* ranges from Oxfordian-Kimmeridgian to Aptian (Fig. 10).

Sample No. sy 55 (chert): *Praeconosphaera* cf. *sphaeraconus* and *Pseudodictyomitra* aff. *lanceloti* were obtained from a chert clast (Fig. 9 and Plate 1). *Pr. sphaeraconus* indicates Oxfordian to Cenomanian while the specimen *Pd.* aff. *lanceloti* is very similar to *Pd.* aff. *lanceloti* described in Baumgartner *et al.* (1995a, b) from the Barremian. The clast is therefore assigned to the Barremian (Fig. 10).

Sample No. sy 58 (chert): A chert clast yielded *Homoeoparonaella* sp., *Pseudodictyomitra leptoconica*, *Pantanellium squinaboli*, *Spongotripus* (?) sp. and Archaeodictyomitridae gen. et sp. indet. (Fig. 9 and Plate 1). *Pd. leptoconica* is Late Barremian to Early Aptian and *Pt. squinaboli* is Kimmeridgian-Tithonian to Aptian (Baumgartner *et al.*, 1995a, b). The specimen of Archaeodictyomitridae gen. et sp. indet. is similar to *Thanarla carboneroensis* described in O'Dogherty (1994) which ranges from Barremian to Aptian. The gravel is therefore assigned to Late Barremian to Early Aptian (Fig. 10).

(4) Locality E

Sample No. sy 20 (chert): A chert clast yielded *Pantanellium oligoporum* and *Poulpus* sp. (Fig. 9 and Plate 1). Hori (1999) described *Pt. oligoporum* as a species ranging from Oxfordian to Berriasian (Fig. 10).

Sample No. sy 29 (chert): *Mirifusus* sp. cf *dianae* was obtained form a chert clast (Fig. 9 and Plate 1). Baumgartner *et al.* (1995a, b) suggests that this species is from the Bathonian to Hauterivian (Fig. 10).

Sample No. sy 25 (chert) and Sample No. sy 32 (silicified rock): Foraminifera were obtained from a each samples. Sample No. sy 25 co-yield abundant radiolarian fossils.

DISCUSSION

Along the length of the River Euphrates, there is a basement of rocks including Precambrian gneiss and schist, upper Paleozoic to lower Triassic schist, Paleozoic to Mesozoic marble and schist, Triassic to Cretaceous neritic limestone, Cretaceous clastic and carbonate rocks, Cretaceous to Paleocene volcanic and sedimentary rocks, Cretaceous basalt, Mesozoic ophiolite, upper Cretaceous pelagic limestone and radiolarian chert. This basement is covered by Cenozoic sedimentary and volcanic rocks in the Taurides (Geological Survey of Turkey, 1963, 1966, 1975, 1989, and 2002a, b, and c). By contrast, in the Arabian platform, Cenozoic sedimentary and carbonate rocks and basalts are widely exposed.

Thus the clasts of chert and the plutonic and metamorphic rocks in the gravel beds are likely to have originated in the eastern Taurides, SE Turkey, since there is no exposure of those rocks on the Arabian platform (Geological Survey of Turkey, 1963; Bundesanstalt für Geowissenschaften und Rohstoff and UNESCO, 1998). Since Cenozoic felsic volcanic rocks are distributed along the River Euphrates in the Taurides (Geological Survey of Turkey, 1963), clasts of rhyolite and tuffaceous rocks will have originated from these formations. The clasts of silicified rock resemble the silicified felsic tuff intercalations in Neogene gypsum on the Arabian platform in having fossils such as foraminifera, bivalves etc. (Fig. 8g) and in addition, some include many crystals of plagioclase. These clasts are likely to have been derived from the silicified Neogene felsic tuff.

The geologic units that include radiolarian chert are exposed as small bodies only to the west and northeast of Adiyaman, Çermik and to the north of Dadas along the River Euphrates (Geological Survey of Turkey, 2002a, b, and c). The chert bodies have traditionally been assigned to the Upper Cretaceous (e.g. Geological Survey of Turkey, 1975), although not on fossil evidence. The present study has revealed that the chert clasts, which form the major component of the Quaternary gravel beds, are Middle Jurassic to Early Cretaceous in age. But, in addition, these beds include clasts of Jurassic radiolarian chert, which has not previously been reported from the eastern Taurides. These facts suggest that the chert bodies exposed in the higher reaches of the stream are not Upper Cretaceous but in reality Jurassic to Lower Cretaceous, otherwise Jurassic to Lower Cretaceous chert bodies exposed together with the Upper Cretaceous ones were eroded out.

Radiolarian chert that does not include terrigenous clastics is generally considered to have been formed at the bottom of oceans at sites where two conditions are satisfied: (1) they are below the carbonate compensation depth (CCD), and (2) are distant from the continent which provides the terrigenous clastics. This means that radiolarian chert is an indicator of an ancient deep and pelagic environment. The co-occurrence of foraminifera in radiolarian chert samples 5 and 25 may suggest sedimentation in an environment which was above the CCD but still not out of range of deposition from a continental source during the Middle Jurassic to Early Cretaceous periods.

ACKNOWLEDGMENTS

Drs Bassam Jamous and Michel Al-Maqdissi of the Syrian Directorate General of Antiquities and Museums kindly allowed us to carry out our study in Ar-Raqqa Prefecture. Mr Ibrahem Khalil of Raqqa Museum helpfully assisted us to carry out the field survey. Dr Giles Clarke read the manuscript and gave us valuable comments. This study was supported by the Grant in Aid for Scientific Research on Priority Area from the MEXT, Japan. To all of these we would like to express our gratitude.

REFERENCES

Al-Riyami, K., Danelian, T. and Robertson, A.H.F. (2001) Rdiolarian biochronology of Mesozoic deep-eater successions in NW Syria and Cyprus: implications for south-Tethyan evolution. *Terra Nova*, **14**, 271–280.

Baumgartner, P.O. (1980) Late Jurassic Hagiastridae and Patulibracchiidae (Radiolaria) from the Argolis Peninsula (Peleponnesus, Greece). *Micropaleontology*, **26**, 274–322.

Baumgartner, P.O., O'Dogherty, L., Gorican, S., Dumitrica-Jud, R., Dumitrica, P., Pillevuit, A., Urquhart, E., Matsuoka, A., Danelian, T., Bartolini, A., Carter, E.S., De Wever, P., Kito, N., Marcucci, M. and Steiger, T. (1995a) Radiolarian Catalogue and systematics of Middle Jurassic to Early Cretaceous Tethyan genera and species. In Baumgartner, P.O., O'Dogherty, L., Gorican, S., Urquhart, E., Pillevuit, A., and De Wever, P. (Eds.) Middle Jurassic to Lower Cretaceous Radiolaria of Tethys: Occurrence, Systematics, Biochronology. Mémoires de Géologie (Lausanne) 23, 37–685.

Baumgartner, P.O., Bartolini, A., Carter, E.S., Conti, M., Cortese, G., Danelian, T., De Wever, P., Dumitrica, P. Dumitrica-Jud, R., Gorican, S.,Guex, J., Hull, D.M., Kito, N., Marcucci, M., Matsuoka, A., Murchey, B., O'Dogherty, L., Savary, J., Vishnevskaya, V., Widz, D. and Yao, A. (1995b) Middle Jurassic to Early Cretaceous Radiolarian Biochronology of Tethys based on Unitary Associations. In Baumgartner, P.O., O'Dogherty, L., Gorican, S., Urquhart, E., Pillevuit, A., and De Wever, P. (Eds.) Middle Jurassic to Lower Cretaceous Radiolaria of Tethys: Occurrence, Systematics, Biochronology. Mémoires de Géologie (Lausanne) 23, 1013–1048.

Beccaletto, L., Bartolini, A.-C., Martini, R., Hochuli, P.A. Kozur, H. (2005) Biostratigraphic data from Çtemi Mélange, northwest Turkey: Palaeogeigraphic and tectonic implications. *Palaeogeigraphy, Palaeoclimetology, Palaeoecology*, **221**, 215–224.

Bozkurt, E., Holdworth, B.K. and Ali Koçyi. G. (1997) Implications of Jurassic chert identified in the Tokat Complex, northern Turkey. *Geol. Mag.*, **134**, 91–97.

Bundesanstalt für Geowissenschaften und Rohstoff and UNESCO (1998) International Geological Map of Europe and the Mediterranean Regions 1:500000.

Clark, B.L. and Campbell, A.S. (1942) Eocene radiolarian faunas from the Monte Diablo area, California. Geological Society of America Special Paper 39, 1–112.

Demirtasli, E. (1984) Stratigraphy and tectonics of the area between Silifke and Anamur, Central Taurus mountains. In Tekeli, O. and Göncüoglu, M.C. (Eds.) Proceedings of the International Symposium on the Geology and the Taurus Belt, 101–118.

Danelian, T., Robertson, A.H.F., Collins, A.S. and Poisson, A. (2006) Biochronology of Jurassic and Early Cretaceous radiolarites from the Lycian Melange (SW Turkey) and implications for the evolution of the Northern Neotethyan ocean. In Robertson, A.H.F. and Mountrakis, D. (Eds.) Tctonic Development of the Eastern Mediterranean Region. Geological Society of London Special Publication 260, 229–236.

Dewey, J.F., Hempton, M.R., Kidd, W.S.F., Saroglu, F. and Şengör, A.M.C. (1986) Shortening of continental lithosphare: the neotectonics of eastern Anatolia –a young collision zone. Geological Society of London Special Publication 19, 3–36.

De Wever, P., Sanfilippo, A. and Riedel, W.R. and Gruber, B. (1979) Triassic Radiolarians from Greece, Sicily and Turkey. *Micropaleontology*, **25**, 75–110.
De Wever, P., Dumitirica, P., Caulet, J.P., Nigrini, C. and Caridroit. M. (2001). Taxonomy of Radiolaria. *In* De Wever, P., Dumitirica, P., Caulet, J.P., Nigrini, C. and Caridroit. M. eds., Radiolarians in the Sedimentary Record, 79–285, Gordon and Breach Science Publishers, Amsterdam.
Geological Survey of Turkey (1963) Explanatory Text of the Geologic Map of Turkey 1:500000 [ERZURUM].
Geological Survey of Turkey (1966) Explanatory Text of the Geologic Map of Turkey 1:500000 [SIVAS].
Geological Survey of Turkey (1975) Explanatory Text of the Geologic Map of Turkey 1:500000 [HATAI].
Geological Survey of Turkey (1989) Geologic Map of Turkey 1:2000000.
Geological Survey of Turkey (2002a) Geologic Map of Turkey 1:500000 [ERZURUM].
Geological Survey of Turkey (2002b) Geologic Map of Turkey 1:500000 [HATAI].
Geological Survey of Turkey (2002c) Geologic Map of Turkey 1:500000 [SIVAS].
Göncüoglu, M.C., Kawahara, K., Tekin, U.K. and Turhan, N. (2004) Upper Permian (Changxingian) Radiolarian Cherts within the Clastic Successions of the Karakaya Complex in NW Anatolia. *Turkish Journal of Earth Sciences*, **13**, 201–213.
Göncüoglu, M.C. and Turhan, N. (1984) Geology of Bitlis metamorphic belt. In Tekeli, O. and Göncüoglu, M.C. (Eds.) Proceedings of the International Symposium on the Geology and the Taurus Belt, 237–244.
Göncüoglu, M.C., Yaliniz K.M. and Tekin, U.K. (2006) Geochemical features and radiolarian ages of volcanic rocks from the Izmir-Ankara suture belt, western Turkey. International Symposium on Mesozoic ophiolite belts of Northern Part of the Balkan Peninsula, abstract volume, 41–44.
Hall, R. (1976) Ophiolite emplacement and evolution of the Taurus suture zone, SE Turkey. *Bulletin of Geological Society of America*, **87**, 1078–1088.
Hori N. (1999) Latest Jurassic radiolarians from the northeastern part of the Torinoko Block, Yamizo Mountains, central Japan. *Science reports of the Institute of Geoscience, University of Tsukuba. Section B, Geological sciences 20*, 47–114.
Hori, N., Saito, M. and Toshimitsu, S. (2002) Late Jurassic radiolarian fauna from the Ikenohara Formation of the Kurosegawa Belt in the Toyo-Izumi area, Kumamoto Prefecture, Kyushu, Japan. *Bulletin of the Geological Survey of Japan*, **53**, 689–724.
Hoshino, M., Tanaka, T., Nakamura, T., Yoshida, H., Saito, T., Tsukada, K., Katsurada, Y., Aoki, Y. and Oho, S. (2010) Geological and chronological study in the Bishri region. *AL-RĀFIDĀN, Special Issue 'Formation of tribal communities: Integrated research in the middle Euphrates, Syria*, 9–19.
Mekik, F.A. (2000) Early Cretaceous Pantanelliidae (Radiolaria) from Northwest Turkey. *Micropaleontology*, **46**, 1–30.
Ministry of Industry, S.A.R. (1964) Geological Map of Syria I-37-XXII.
Murat, E. (1993) Geological outline of Anatolian Peninsula. *Chitsu News*, No. 467, 11–20 (In Japanese).
Nikita Y.B. and Tekin, U.K. (1996) Age of radiolarian-chert blocks from the Senonian Ophiolitic Melange (Ankara, Turkey). *The Island Arc*, **5**, 114–122.
Ohnuma, K., Fujii, S., Nishiaki, Y., Tsuneki, A, Miyashita, S. and Sato, H. Eds. (2008) Integrated research in the Bishri Mountains on the middle Euphrates, News Letter of the Grant-in-Aid for Scientific Research on Priority Area from MEXT, Japan, 'Formation of Tribal Communities in the Bishri Mountains, middle Euphrates' No. 10.
Okey, A.I. (1984) Distribution and characteristics of the northwest Turkish blueschists. In Dixon, J.E. and Robertson, A.H.F. (Eds.) The Geological Evolution of the Eastern Mediterranean, Geological Society of London Special Publication 17, 455–466.
Okey, A.I. (1985) High pressure/low temperature metamorphic rocks of Turkey. In Ewans, B.W. and Brown, E.H. (Eds.) Bulueschists and Eclogites, *Memoir of the Geological Society of America*, No. 164, 147–154.

O'Dogherty, L. (1994) Biochronology and paleontology of Mid-Cretaceous radiolarian from Northern Apennines (Italy) and Betic Cordillera (Spain). Mémoires de Géologie (Lausanne) 21, 1–415.

Ozgul, N. (1984) Stratigraphy and tectonic evolution of the Central Taurides. In Tekeli, O. and Göncüoglu, M.C. (Eds.) Proceedings of the International Symposium on the Geology and the Taurus Belt, 77–90.

Pessagno, E.A. (1973) Upper Cretaceous Spumellariina from the Great Valley Sequence, California Coast Ranges. *Bulletins of American Paleontology*, **63**, 49–102.

Pessagno, E.A. (1977) Lower Cretaceous radiolarian biostratigraphy of the Great Valley Sequence and Franciscan Complex, California Coast Ranges. Cushman Foundation for Foraminiferal Research, Special Publication 15, 1–87.

Robertson. A.H.F. (2002) Development of concepts concerning the genesis and emplacement of Tethyan ophiolites in the Eastern Mediterranian and Oman regions. *Earth-Science Review*, **66**, 331–387.

Robertson, A.H.F. and Woodcook, N.H. (1981) Godene zone, Antalya Complex, SE Turkey: volcanism and sedimentation of Mesozoic marginal ocean crust. *Geologische Rundschau*, **70**, 1177–1214.

Şengör, A.M.C. (1979) Mid-Mesozoic closure of Permo-Triassic Tethys and its implications. *Nature*, **279**, 590–593

Şengör, A.M.C. and Yilmaz, Y. (1981) Tethyan evolution of Turkey: A plate tectonic approach. *Tectonophysics*, **75**, 181–241.

Tekeli, O., Aksay, A., Urgun, B. and Isik, A. (1984) geology of the Aladog mountains. In Tekeli, O. and Göncüoglu, M.C. (Eds.) Proceedings of the International Symposium on the Geology and the Taurus Belt, 143–158.

Tekin, U.K. and Göncüoglu, M.C. (2008) Late Middle to Early Late Triassic radiolarian faunas from the Izmir-Ankara Suture belt in western Turkey: Remarks on the evolution of the Neotethyan Izmir-Ankara ocean. *Berichte Geol. B.-A.*, **76**, 59–60.

Tekin, U.K. and Göncüoglu, M.C. (2009) Late Middle Jurassic (Late Bathonian-Early Callovian) Radiolarian Cherts from the Neotethyan Bornova Flysch Zone, Spil Mountains, Western Turkey. *Stratigraphy and Geological Correlation*, **17**, 298–308. Published in Russian in *Stratigrafiya. Geologicheskaya Korrelyatsiya*, **17**, 70–80.

Tekin, U.K., Göncüoglu, M.C. and Turhan, N. (2002) First evidence of Late Carnian radiolarians from the Izmir–Ankara suture complex, central Sakarya, Turkey: implications for the opening age of the Izmir–Ankara branch of Neo-Tethys. *Geobios*, **35**, 127–135.

Woodcook, N.H. and Robertson, A.H.F. (1982) Wrench and thrust tectonics along a Mesozoic-Cenozoic continental margin: Anatolia Complex, SW Turkey. *Jour. Geol. Soc. London*, **139**, 147–163.